frontiers in Materials

ORIGINAL RESEARCH
published: 22 January 2021
doi: 10.3389/fmats.2020.615021

Fluidic Platforms Incorporating Photo-Responsive Soft-Polymers Based on Spiropyran: From Green Synthesis to Precision Flow Control

Komala Pandurangan, Ruairi Barrett, Dermot Diamond and Margaret McCaul**

Insight Centre for Data Analytics, National Centre for Sensor Research, Dublin City University, Dublin, Ireland

In this paper, we describe how to create simple fluidic systems incorporating soft polymer actuator valves, that can provide highly precise control of flow rates in fluidic channels as an example of a 4D-materials based platform. The particular approach we describe employs photoresponsive gels that swell/contract via a light stimulus, enabling flow behavior to be controlled from outside the fluidic platform in a completely remote and non-contact manner. An improved synthesis of the spiropyran molecular photoswitch that delivers high yields (77%) using scalable green chemistry is described, along with details on how to build the valve structures in custom designed sites within the fluidic system. Fabrication of a demonstrator fluidic system incorporating up to four valves is described, along with electronics and in-house developed PID control software for achieving precise control of flow in the channels using LEDs. The resulting system demonstrates an innovative approach to microfluidics that offers scalability in terms of the number of polymer actuators along with wide variability of actuator form and function.

Keywords: green synthesis, microfluidics, stimuli-responsive gels, actuators, sensors, flow-control, soft-valves

OPEN ACCESS

Edited by:
Frank Alexis,
Yachay Tech University, Ecuador

Reviewed by:
Xuan Shouhu,
University of Science and Technology of China, China
Francisco M. Raymo,
University of Miami, United States

****Correspondence:***
Dermot Diamond
dermot.diamond@dcu.ie
Margaret McCaul
margaret.mccaul@dcu.ie

Specialty section:
This article was submitted to Smart Materials, a section of the journal Frontiers in Materials

Received: *07 October 2020*
Accepted: *11 December 2020*
Published: *22 January 2021*

Citation:
Pandurangan K, Barrett R, Diamond D and McCaul M (2021) Fluidic Platforms Incorporating Photo-Responsive Soft-Polymers Based on Spiropyran: From Green Synthesis to Precision Flow Control. Front. Mater. 7:615021. doi: 10.3389/fmats.2020.615021

INTRODUCTION

Society is set to be transformed by the impact of breakthroughs emerging from fundamental materials science and engineering. We are on the cusp of a profound change in our ability to create devices with performance characteristics far beyond that of existing technologies that will affect all aspects of our lives—from personal health, to agriculture and food production, to protecting the status of our environment, to energy generation/storage and efficient use, to everyday products. At the heart of this change is the ability to fabricate 3D structures at scales from nano to macro, coupled with the impact of stimuli-responsive materials that provide the fourth-dimension effect, i.e., time-based changes in 3D order due to the influence of localized stimuli. The incorporation of stimuli-responsive behavior into 3D materials will open multiple opportunities to develop next generation technologies across these broad application domains, particularly when the response can be managed through feedback loops. We are particularly interested in the application of these ideas in microfluidic platforms, as this could open the way to significant advances in an array to technologies allied with 3D tissue and organ engineering, new approaches to *in-situ* molecular sensing (biosensors, chemical sensors) for personal health and environmental monitoring, and new concepts in drug delivery.

In this paper, we present a complete methodology for preparing a simple multichannel fluidic platform in which the flow behavior can be precisely controlled from outside using light through the

incorporation of photoresponsive soft-gel actuators based on spiropyrans. Spiropyrans are a unique class of organic molecules well-known for their striking photochromic behavior (Klajn, 2014) due to reversible first order photoinduced structural isomerization between closed spiropyran (SP) and open merocyanine forms (MC) (Keum et al., 1994; Minkin, 2004; Seefeldt et al., 2010; Xia et al., 2017). The molecular transformation can be triggered by various stimuli including temperature (Fischer and Hirshberg 1952), solvent polarity (Rosario et al., 2002), mechanical force (Lee et al., 2013; Vidaysky et al., 2019), redox potential (Wagner et al., 2011), light (Matczyszyn et al., 2015) and pH (Keum et al., 1994). This switchable behavior has been explored for a wide range of applications such as data storage (Kawata and Kawata, 2000), photo-responsive materials (Sun et al., 2016; Li et al., 2016; Schiphorst et al., 2016; Dou et al., 2017; Campos et al., 2018; Wang et al., 2019), drug delivery (Kocer et al., 2005; Chen et al., 2016; Jalani et al., 2016; Karimi et al., 2017), soft robotics (Xie et al., 2012; Li et al., 2016; Abdollahi et al., 2017), sensors (Byrne and Diamond 2006; Shao et al., 2010; Zhang et al., 2019a), and soft actuators (Sugiura et al., 2007; Florea et al., 2012; Ziolkowski et al., 2013; Czugala et al., 2014; Dunne et al., 2016a; Ziółkowski et al., 2016; Coleman et al., 2017). Spiropyran incorporated light responsive hydrogels have been successfully demonstrated to function as photoresponsive valves in microfluidics (Sugiura et al., 2009; Schiphorst et al., 2015; Schiphorst et al., 2018). Hydrogel based actuators and photo-responsive soft-polymer valves are of particular interest in this respect due to their inherently biomimetic characteristics, compared to the commonly used hard-materials based commercial microvalves. Spiropyran derivatives with appropriate function can be successfully incorporated to *P*-NIPAM with a suitable crosslinker and a photo initiator and photopolymerized in the desired shape and location in channels to enable flow regulation using light (Satoh et al., 2011; Delaney et al., 2017).

While the concept and platform may appear relatively simple, producing and validating these ideas in a typical research group is far from easy, as it requires the involvement of a team of researchers whose expertize ranges from synthetic chemistry, through 3D printing, microfluidics, photonics, stimuli-responsive soft materials, and computer coding. Mobilizing this breadth of expertize in a coherent effort is challenging but essential if the tremendous potential of this change is to be realized. Those who can assemble this expertize in breadth and depth will lead the way forward for others to follow. It is our hope that this paper will inspire other groups to travel along this very exciting pathway.

MATERIALS AND METHODS

Overall Strategy

Making a fluidic platform in which the flow is controlled by light requires a number of contributions to be individually created, and subsequently combined in an appropriate manner to produce the complete functional demonstrator. These contributions can be summarized as follows;

- Synthesis of the molecular photoswitch (based on spiropyrans) that will convey photoresponsive behavior to the gel actuator. In this paper, we present a significantly improved synthetic route consistent with the principles of green chemistry while also capable of scale-up.
- Production of the fluidic system, and consequent incorporation of the gel actuators into channels using *in-situ* photopolymerisation.
- Production of a platform for directing light efficiently to the actuator locations to enable effective *in-situ* photopolymerization of the valve structures and their subsequent switching for effecting flow control.
- Implementing a control system based on real-time measurement of the control parameter (flow) while varying the intensity of the control stimulus (light) according to a feedback algorithm (e.g., PID control) which enables a set flow rate to be reached quickly and maintained accurately.

Creation of even relatively simple demonstration platforms requires knowledge ranging across synthetic chemistry, materials chemistry, materials engineering, optics and electronics, programming and analytical chemistry. While this was challenging in the past, it is becoming more accessible to research groups due to the increasingly multidisciplinary character of modern research, and this trend is certain to strengthen into the future. In the following sections, we provide more detailed context for these contributions that together can provide the foundation for many emerging ideas and concepts with very broad impact potential.

Photoswitch Molecular Design Considerations and Synthesis

As the molecular photoswitch used to impart the photoswitchable behavior to the gel is not available commercially, it must be synthesized. The synthetic route for producing the photoswitch must be scalable, based on readily available, low-cost precursors, and consistent with the principles of green chemistry. Herein, we present a new optimized synthetic method for the synthesis of spiropyran in gram quantities that meets these requirements and can be used for the production of relatively large quantities of photoresponsive soft gels at low cost. Spiropyran (SP) with hexyl acrylate on the SP ring (SP-8-hexyl acrylate, **Figures 1A**, **2**) exhibits efficient photo switching while covalently incorporated within a p-NIPAM hydrogel, particularly when substituted at the 8' position (Dunne et al., 2016b). The length of the alkyl chain spacer appears to play a significant role in providing effective reversible gel expansion and contraction. N-hexyl linkers provide an optimum greater degree of conformational flexibility within the polymeric hydrogel which facilitates the molecular rearrangement during isomerization (Klajn 2014; Chen et al., 2016). Furthermore, the photo switching behavior appears unaffected by the polymerization conditions commonly used to create these gels, which is a critical consideration for creating effective actuators (Delaney et al., 2017). Furthermore, the absence of a nitro group para to the pyran oxygen means that

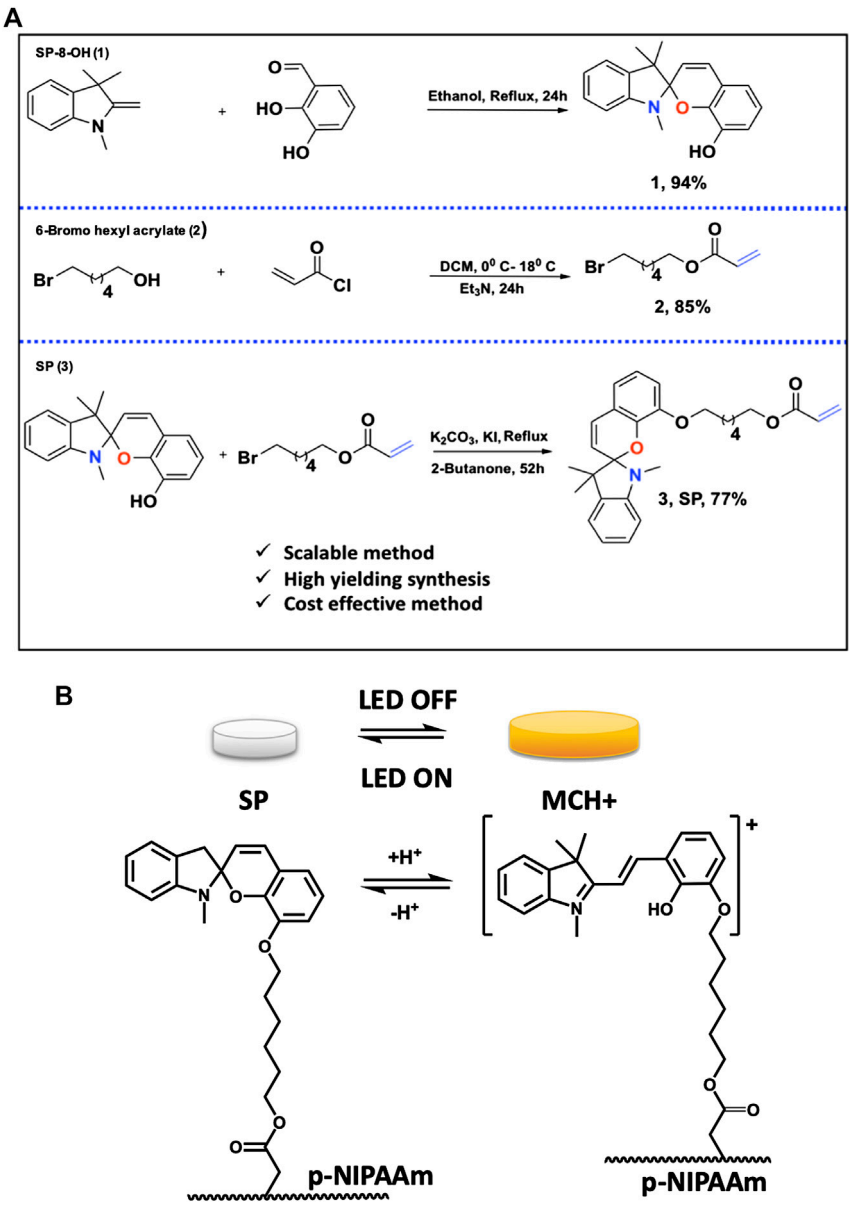

FIGURE 1 | (A) Synthesis of SP-8-OH 1); 6-Bromo hexyl acrylate 2) and SP 3); **(B)** In the absence of light, the protonated merocyanine isomer is predominant (MCH^+, charged, yellow) and the gel is hydrated and expanded. Illumination with the 450 nm LED triggers switching to the spiropyran isomer (SP, uncharged colourless) and the gel contracts as water is expelled. When the LED is switched off, the SP isomer is spontaneously reformed, and the gel reverts to the expanded form. See also **Supplementary Video S1**.

under acidic conditions, the equilibrium (**Figure 1B**) will spontaneously favor formation of the protonated merocyanine, and the hydrogel will naturally assume the expanded (valve closed) form in the absence of light. The rapid spontaneous reversion to the protonated merocyanine is additionally attractive as it can speed up the kinetics of gel reswelling, which tends to be significantly slower than contraction. The reswelling process depends on both the photoswitch kinetics (often rate determining for the overall reswelling process), the hydrogel composition and the nature of diffusion. With this particular derivative, the formation of the protonated merocyanine is very fast, to the extent that it is no longer rate determining for reswelling (Schiphorst et al., 2015), which is a significant advantage for our purposes. Upon illumination (in this case with a 450 nm LED), the equilibrium shifts to favor the uncharged spiropyran, which triggers gel contraction and valve opening. This has the added advantage for our purposes in the only one LED is required to control the valve status.

The synthetic method involves synthesis of SP in three-steps from commercially available 6-bromohexanol. Each step of the synthesis was optimized in terms of solvent, reaction time, catalyst and base, to produce precursors SP-8-OH 1),

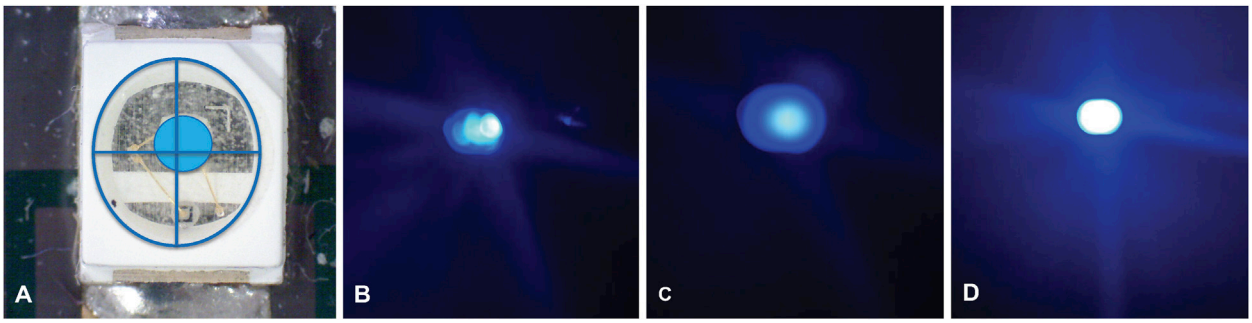

FIGURE 2 | Images showing **(A)**: Off-centred surface mount LED. Comparison of light dispersion using the SM LED 1.75 × 1.0 mm elliptical photomask and **(B)**: one-layer PMMA diffuser, **(C)**: two-layer PMMA diffuser and **(D)**: three-layer PMMA diffuser.

TABLE 1 | Optimized reaction conditions for **1–3**, **Figure 1A**.

Entry	Solvents	Base	Catalyst/eq.	Temp°C/Time (h)	Yield (%)
SP-OH (1)					
1	Ethanol	-	-	78°C/6 h	84
2	Ethanol	-	-	78°C/24 h	94
6-Bromohexyl acrylate (2)					
3	DCM	Et_3N	-	0°–18°C/0–17 h	42
4	DCM	Et_3N	-	0°–18°C/0–24 h	85
SP (3)					
5	2-Butanone	K_2CO_3	KI (0.1)	80°C/15 h	55
6	2-Butanone	K_2CO_3	KI (1.0)	80°C/52 h	77

Bold values refers to the three reaction steps in Figure 1A, indicated in parentheses after SP-OH (1); 6-bromohexyl acrylate (2) and SP (3), and in the yields, Figure 1A.

TABLE 2 | Effect of solvent on the synthesis of SP (3), **Figure 1A**.

Entry	Solvents	Base	Catalyst/ eq.	Temperature (°C)	Time (h)	Yield (%)[a]
1	Acetone	K_2CO_3	KI (1)	56	52	15
2	THF	K_2CO_3	KI (1)	66	52	[b]
3	CH_3CN	K_2CO_3	KI (1)	82	24	20
4	Methanol	K_2CO_3	KI (1)	64	6	[b]

[a]*Isolated yield.*
[b]*No product formation, starting materials recovered.*

6-bromohexyl acrylate 2) and SP 3), **Figure 1A**. Precursors SP-8-OH and 6-bromohexyl acrylate were obtained in 85%/94% yields, respectively, and the desired SP in 77%. The most common method for the synthesis of spiropyran derivatives involves condensation of indoline or 2-methyl indolium salt with the corresponding salicylaldehyde in alcohol, basic alcohol and ketonic solvents (Lukyanov and Lukyanova 2005; Balmond et al., 2016; Ozhogin et al., 2019). SP-8-OH was previously prepared in moderate yields by condensation of indoline/2-methylindolium salt with 2,3-dihydroxy salicylaldehyde in basic ethanol/acetonitrile (Zhang et al., 2019b). Bases such as triethylamine and piperidine were employed to prevent the formation of the di-condensed cyclic product rather than the desired mono-condensed spiropyran. In contrast, we employed a novel base-free mechanism to synthesize SP-8-OH, by reacting 1,3,3-trimethyl-2-methyleneindoline (Fischer base) with 2,3-di-hydroxy benzaldehyde in ethanol, **Figure 1A**.

After 6 h reflux, this afforded SP-8-OH 1) selectively with a yield of 84% without any side products. Prolonging the reaction up to 24 h further enhanced the yield of SP-8-OH 1) to 94% after simple chromatographic purification (due to lower amounts of impurities), see **Table 1**.

In the second step, 6-bromohexyl acrylate 2) was synthesized in 42% yield from 6-bromo hexanol and acryloyl chloride using triethylamine as a base. Increasing the proportion of base to 1.6eq and increasing the reaction time to 24 h, enhanced the reaction and the product was recovered smoothly in 85% yield.

In the final step of the synthesis, SP 3), which is the desired photo-responsive unit for creating the gel photoactuators, was prepared by reacting 1 and 2 (**Figure 1A**) in the presence of potassium carbonate using potassium iodide as a catalyst, **Table 1**. Both the catalyst and base provide optimum basicity in 2-butanone during the substitution of 6-bromohexyl acrylate with SP-8-OH. Under the initial conditions (see entry 6, **Table 1**) SP 3) was produced in 57% yield. Altering the solvent/catalyst equivalent composition to 1.0 and extending the reaction time to 52 h afforded SP 3) in an enhanced yield of 77%. Subsequently, acetone, acetonitrile, THF and methanol were substituted for 2-butanone, to examine their effect on the synthesis of SP 3), **Table 2**. Acetone generated SP in lower yield in comparison to 2-Butanone, whereas more polar solvents such as acetonitrile and methanol generated either less SP or no SP (entry 3 and 4 in **Table 2**). Lower yields of ca. 20% were obtained when acetonitrile was employed as a solvent. In contrast, methanol produced indoline, the starting material of SP-8-OH suggesting decomposition of 1 under the reaction conditions employed (Han and Chen 2011; Tan et al., 2006; Yagi et al., 2009; Chen et al., 2014).

Higher yields of SP were obtained only in the case of moderately polar 2-butanone, wherein the base and catalyst together appear to provide the optimum conditions for the substitution of 6-bromohexyl acrylate with SP-8-OH to proceed effectively. To utilize the scope of the developed synthetic method, we further developed the methodology to synthesize SP in larger gram scales. Each step of the synthesis outlined in **Figure 1A**, was carried out easily in larger scale to

determine the feasibility of the reaction to produce SP in much similar yields. This methodology produced SP 3) and precursors (1–2), in similar yields and coupled with simple chromatographic purification due to low levels of impurities, gram quantities of pure SP were easily obtained.

Fabrication of the Photoresponsive Hydrogel Valve

Gel Cocktail Composition

The monomeric cocktail was prepared using 200 mg NIPAAm, 8.35 mg crosslinker MBIS (3 mol% relative to NIPAAm), 7.91 mg SP (1 mol% relative to NIPAAm), 7.42 mg photoinitiator PBPO (1 mol% relative to NIPAAm) and 6.05 μL Acrylic Acid AA (5 mol% relative to NIPAAm) dissolved in 500 μL 2:1 v/v THF: DI water.

We compared two techniques to create microfluidic platforms incorporating the soft polymer valve structures, i.e., laser ablation [(e.g., Epilog Zing 16)], micro-milling (Datron CAT3D-M6), and 3D Printing (DWS SLA 3D Printer). For laser ablation and micro milling the fluidic chip design contained four fluidic channels with an inlet, outlet and an anchor structure for the valve which were rastered or micro milled into a 2 mm thick PMMA bottom layer with a similar 2 mm PMMA layer acting as a capping and sealing layer. These two layers were bonded together using the thermal bonding procedure outlined by Donohoe et al. (Donohoe et al., 2019), after which the fluidic connection ports (barbs) were manually glued in place to accommodate the 1/16" tubing.

Creation of the Photoresponsive Hydrogel Valve Structures

The monomer cocktail described above was introduced to the fluidic channel using a syringe. Once the fluidic channel was filled with the cocktail, the interconnects were sealed to prevent any movement of liquid. Polymerization was achieved using blue surface-mounted LEDs (Kingbright HB Blue 450 nm, 600 mW/4.5 lm/1.3 cd, 3.5 V) at 450 nm wavelength and 20% power for 60 s through a 1.75 × 1.0 mm elliptical photomask made from 1 mm thick opaque PMMA (55 × 65 mm) with through-holes of the desired shape and size milled out and aligned with the LED. This provided optical pathways from the LEDs to the monomer cocktail aligned with the valve anchor points in the fluidic channels. Illumination of the monomer cocktail triggered polymerization of the doughnut-shaped polymer gel valve structure at the desired locations, with the opaque PMMA blocking any stray or scattered light. Under the conditions used, the valve structures are formed in the contracted (open) state, enabling any remaining unpolymerized monomer cocktail to be flushed from the fluidic channels using Milli Q ultrapure water. The polymerized valves were then hydrated using a pH 5 buffer as a proton source and allowed to swell to full size before use. The final composition of the polymer gel is ca. SP 1 mol%, NIPAAm 91 mol%, AA 5 mol%, MBIS 3 mol%. (Ziółkowski et al., 2016). In the swollen gel, the photoswitch exists predominantly in the protonated merocyanine form (MCH+, charged, yellow), whereas in the contracted gel, the spiropyran (SP) form is predominant (**Figure 1B**). Illumination with the 450 nm LED triggers isomerization from MCH + to SP, with simultaneous contraction of the gel and valve opening. When the LED is turned off, SP spontaneously reverts to MCH+ and the valve closes. Note that this means only one LED per valve is required, as valves will revert to the closed state in the absence of light. As switching involves protonation/deprotonation, co-immobilization of AA provides a useful internal proton source/sink to facilitate this isomerization. As the MBIS crosslinks the poly-NIPAAm strands, the amount used is a trade-off between physical robustness and actuation dynamics of the polymer.

Optical Platform and Electronics

The electronic system layout is shown in **Figure 3A**. Digital control of the power to the LEDs was provided via a PCA9685 Pulse Wave Modulation (PWM) controller 1) connected to an Arduino Uno microcontroller 2). An UART serial connection between the Arduino and the laptop was used to enable pre-determined command files to be sent to the PWM. Four Femtobuck constant current drivers 3) were used to control the Kingbright 450 nm LEDs which actuate the polymer valves. To allow for individual control of the polymer valves each driver was connected to a different output of the PWM controller. The system was powered by a 12 V adaptor 4).

It is important to appreciate that even marginal misalignment of the LED, photomask and microfluidic chip can create significant performance issues in the resulting valves, both during valve formation, and subsequent valve control (e.g., failure to block channels completely, failure to reopen properly). The electronic housing and LED platform was therefore designed to facilitate precise alignment of the fluidic chip with the optical sources (LEDs) using notches in the top-plate and chip holder for accurate *in-situ* photo-polymerization of the valve structures, and subsequent reproducible actuation of the photo-responsive valve; i.e. the same optical platform is used to create the polymer valve structures, and for their subsequent actuation (**Figure 3B**).

Another important issue is that surface mount (SM) LEDs commonly produce an off-centre hotspot when illuminated, and this hotspot results in uneven polymerization of the valve structure, **Figure 2A**. To reduce this undesirable effect and improve the reproducibility of the light after LED alignment, an LED diffusor was fabricated using up to three pieces of frosted 2 mm PMMA (55 × 65 mm) placed between the LEDs and the photomask (**Figures 2B–D**). The diffuser was found to disperse the light much more evenly, and effectively removed the hotspot produced by the bare LEDs resulting in more evenly polymerized valves with enhanced shape and size accuracy, see **Figure 4**.

Controlling Flow Using Light

The proportional, integral, differential (PID) control algorithm is broadly applied in engineering for optimizing the behavior of a switching system through variation of respective weighting constants (K_P, K_I, K_D). When switching between set points, a

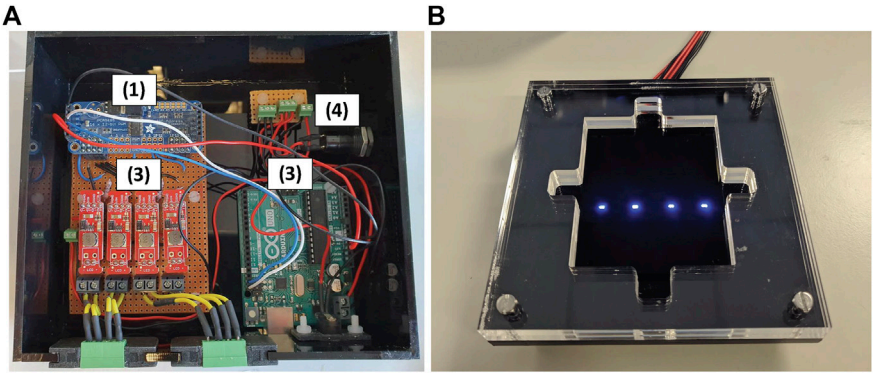

FIGURE 3 | (A) Key components in the Electronics Control System, **(B)** Top plate with notches for alignment of fluidic chip holder. The top plate is attached over the electronics shown in **(A)**.

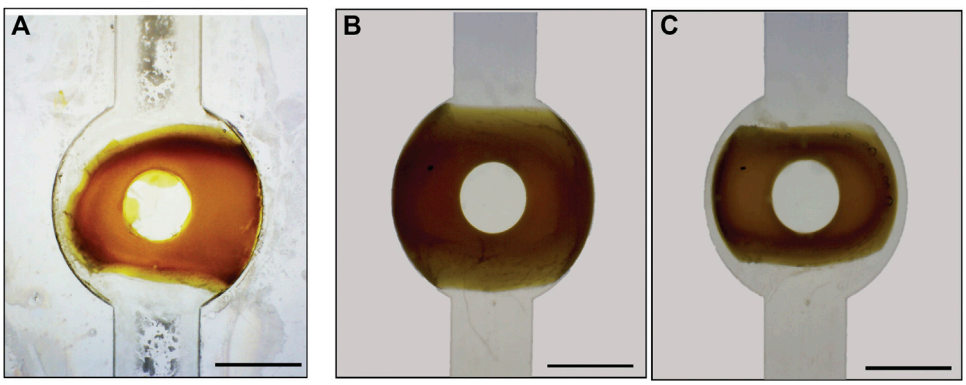

FIGURE 4 | (A) Microscope Image of the soft polymer valve within the fluidic chip before LED hot-spot correction and **(B)** after correction. **(A)** Valve produced without accurate LED alignment around the retention pillar is misshapen and cannot fully close; **(B)** Accurate alignment of the LED coupled with 3-layer diffuser has a much more regular shape nicely centered around the retention pillar within the valve housing feature; **(C)** Exposure to UV-light triggers contraction of the valve allowing flow to occur. The size bar is 1,200 μm.

well-optimized system will minimize overshoots/undershoots, detect and correct for bias, and maximize the switching dynamics.

$$P_{LED} = K_P(F_{SP} - F_M) + K_I \int (F_{SP} - F_M)\mathrm{d}t + K_D\left(\frac{\mathrm{d}(F_{SP} - F_M)}{\mathrm{d}t}\right)$$

where P_{LED} = LED Power input, K_P = Proportional gain (P), K_I = Integral gain (I), K_D = Derivative gain (D) and $(F_{SP} - F_M)$ = Error between the set point flow rate (F_{SP}) and the measured flow rate (F_M). We found that excellent flow control could be obtained using PI control (without the derivative contribution) and differential control was therefore not implemented throughout the study ($K_D = 0$). The PI control algorithm works in the following manner. When the measured flow is much less than the desired (set point) flow ($F_M << F_{SP}$), the differential factor dominates the power setting for the LED (P_{LED}). As the LED power is high, MCH+ is converted to SP and the valve contracts, increasing the flow. As F_M approaches F_{SP}, the LED power reduces proportionally toward a value that will sustain F_{SP}. If $F_M >> F_{SP}$, the converse happens in which the LED is predominantly in the off state, triggering conversion of SP to MCH+, and the valve expands, reducing the flow toward F_{SP}. The dynamic change in flow is determined by the value of K_P – large values produce fast responses, but can also produce large overshoots and oscillations around F_{SP}, rather than a steady, accurate flow. The integral factor corrects for continuous offsets/drift that can arise between F_M and F_{SP} by integrating the difference over a time interval, and gradually increasing or decreasing P_{LED}, depending on whether the offset is negative or positive compared to F_{SP}. The effectiveness depends on the time interval and the value of K_I.

Figure 5 shows the experimental set-up for achieving flow control. The reservoirs A) were filled with milliQ water to different heights (500 and 300 ml) to create a differential pressure for driving pulseless flow from the source to the collection reservoir when the valve was opened. Before connecting the reservoirs to the liquid input/output connectors, the channel was filled manually using a syringe filled with milliQ water to remove air. In this case, the height difference of ~33 mm, produced a head pressure of ~3.23 mbar which was adequate for the system under study. The use of these relatively large fluid volumes in the reservoirs also minimized the

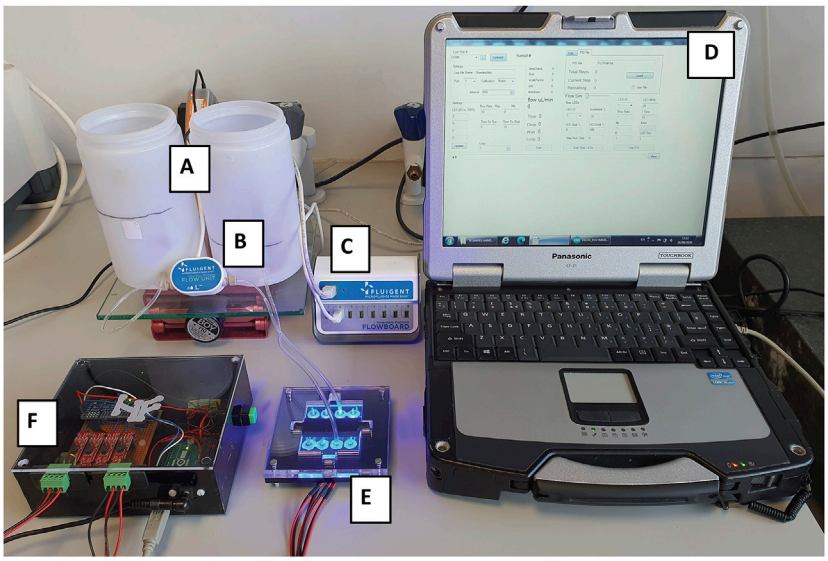

FIGURE 5 | Experimental set-up for achieving PID flow control.

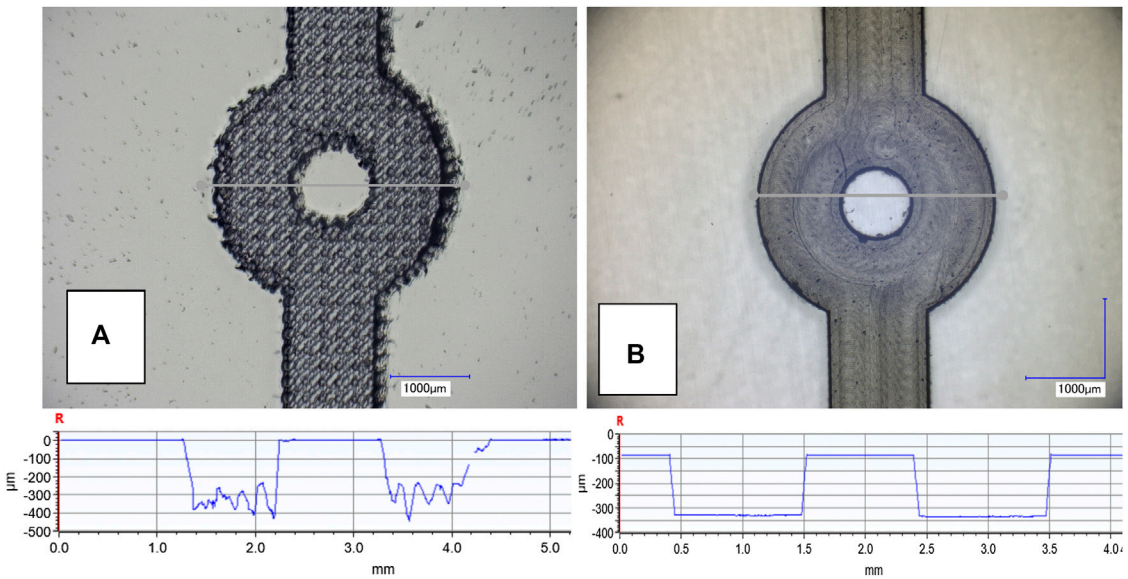

FIGURE 6 | Microscope image of the microfluidic channel and valve retention pillar fabricated using laser ablation **(A)** and micro milling **(B)**, and associated cross sections obtained using optical profilometry. The micro-milled channels give a much smoother final finish with an average surface roughness in the region of 3–5 µm compared to 50–150 µm obtained with laser ablation.

impact of changes in head pressure over time due to fluid transfer. For example, during a typical 24 h experiment, the total volume transferred was ca. 10 ml, and we found this small change in pressure was easily compensated by the PI control algorithm. The system functioned as follows. Liquid flow from the source reservoir A) was monitored continuously using a Fluigent flow sensor B) connected to a Fluigent electronics unit C). The resulting signal was passed to the laptop D), where the PID software algorithm compared the measured flow rate with the set flow rate and varied the control value for the power setting of the LEDs aligned with the polymer valves in the flow system E) via the PWM value in the electronics board F).

RESULTS

In **Figure 6**, microscope images of the valve anchor structure fabricated by laser ablation A) and micro milling B) are

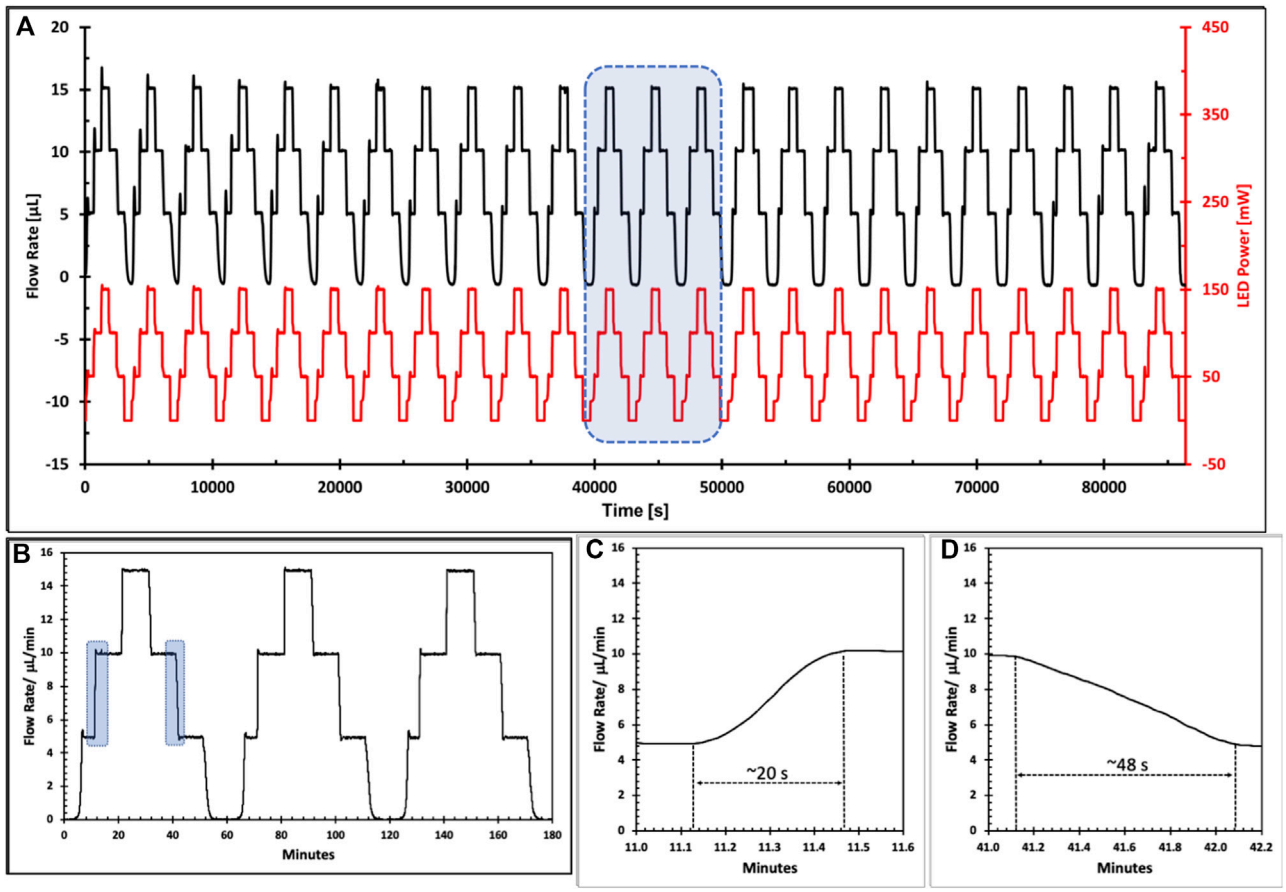

FIGURE 7 | (A) 24 h Continuous Flow Control with a soft polymer valve showing excellent reproducibility over multiple flow rate switching of the sequence 0→5→10→15→10→ 5→0 µL/min (black). The associated LED power switching pattern to generate this flow rate control is shown in red; **(B)** Zoom in on the highlighted section of **(A)** showing detail of three complete flow rate switching sequences illustrating accuracy of the switching between set flow rates and stability of set flow rates. **(C,D)** Indication of the speed of switching between flow rates focusing on the illustrated sections of the first pattern in **(B)**. Increasing flow rate 5→10 µL/min is associated with a contraction of the gel valve and is completed in ca. 20 s; decreasing flow rate 10→5 µL/min is associated with an expansion of the gel valve and is slower at ca. 48 s.

TABLE 3 | Precision and Accuracy of Flow Control (n = 24 for 15 µL/min, n = 48 for 5, 10 µL/min).

Set point (µL/min)	Average SD (µL/min)	Average flow rate (µL/min)	RSD (%)	RE (%)
5	0.063	5.095	1.23	1.90
10	0.059	10.124	0.58	1.24
15	0.061	15.121	0.41	0.80

TABLE 4 | Flow Control Average Response Times for each step (n = 24).

Change in flow rate (µL/min)	Average response times (s)
0 → 5	280
5 → 10	16
10 → 15	11
15 → 10	57
10 → 5	69
5 → 0	183

illustrated. Channels produced using laser ablation exhibited greater channel roughness (in the range 50–150 µm) with associated uneven topography and swarfing compared to micro milling (channel roughness in the range 3–5 µm). **Figure 7** shows the results obtained from 24 replicates of an hour-long switching cycle between 0 and 15 µL/min, in 5 µL/min increments. Each flow rate was maintained for a 10-min period including the response time of the valve. For the 0 µL/min flow rate condition (valve fully swollen), the proportional (K_P) and integral gain (K_I) values were set to 0 to ensure that the LEDs remained fully off. During experiments, it was found that excellent results could be obtained with K_P set in the range 5.0–8.0 and K_I maintained at a value of 0.1.

Table 3 summarizes the precision and accuracy of the flow control over the course of the 24 h experiment. Interestingly, in absolute terms, these are relatively independent of the actual flow

rate, with the average flow rate slightly higher than the set value by ca. +0.1 μL/min, and the standard deviation close to 60 nL/min in all cases. The relatively constant positive offset error for the flow rate suggests that the true error of the system is significantly lower than we report and could be further improved by additional refinement of the PID algorithm, and changes to the valve design and flow system more generally. However, even as it is, these results suggest that the approach as described is already demonstrating very accurate and precise control of flow rate in fluidic channels.

Table 4 compares the response times for each step change in flow rate. Generally speaking, with soft gel structures contraction is faster than expansion, due to the differing dynamics of water release/uptake from the polymer structure (Ziółkowski et al., 2016). This is evident from a comparison of the faster response times for switching 5 → 10 μL/min (16 s) and 10 → 15 μL/min (11 s), with the equivalent 15 → 10 μL/min (57 s) and 10 → 5 μL/min (69 s). At first glance, it appears that complete closure 5 → 0 μL/min (183 s) is significantly faster than initial opening 0 → 5 μL/min (280 s), but this is most likely due to continued swelling of the gel after initial closing which has to be overcome before opening occurs. Much faster valve opening from a completely closed status can be achieved if the gel is pre-dispositioned specifically for this action. An example is provided in the video (**Supplementary Material**), which shows valve opening within a few seconds of exposure to the LED light. Such rapid opening has been demonstrated previously in studies focused on valve opening/closing rather than precise control of flow rate. Our conclusion is that the performance of this system can be significantly improved through further optimization of the multiple facets influencing its response (see *Discussion* below).

DISCUSSION

The synthesis presented above shows that the key component, the spiropyran photoswitch, can be synthesized in high yields using new methods consistent with green chemistry that can be scaled up as needed. Given the small amounts of materials used to create the valve structures, and the compatibility of the gel production with *in-situ* polymerization, it can be concluded that these structures can be produced in large numbers at very low cost within pre-produced fluidic chips. This in turn means that the inclusion of the valves can be achieved post-chip production, and existing manufacturing processes are therefore not affected. The fact that control of the flow system can be affected from outside, using light to trigger responses in responsive structures fully enclosed within the fluidic system is a an attractive proposition, as it means that the fluidics system can be totally isolated from the photonic control source, unlike electronically controlled valves that require physical contacts. This again speaks to the potential for scale up of these actuators within fluidic systems.

Optimization of the valve response is a complex, multifaceted task, involving interplay of multiple factors such as the valve shape, size and design, the optical arrangement for managing interaction of the gel with light, the composition of the gel cocktail, the switching dynamics of the molecular photoswitch, the form and optimization of the control algorithm, and the composition of the external solution. However, even bearing this in mind, it is striking how impressive the results are, even at this early stage of the research. For example, even keeping all other factors as they are, refinement of the control algorithm should result in significant improvements in the flow accuracy. From **Table 3**, the RMS error across the three flow rates is 0.114 μL/min. Optimization of the algorithm should enable most of this constant offset error to be removed. If this alone could be implemented, the resulting RMS error would be close to 0.013 μL/min (i.e., 13 nL/min). However, this would also depend on improving the standard deviation of the steady-state flow rates as well. Improvements in the response time could similarly be affected by considering the response mechanism, involving diffusion into/out of the gel from the surrounding aqueous fluid. This is limited by Fick's law which relates the diffusion rate to the average diffusion pathlength (Porter et al., 2007). For our purposes this means that larger structures take longer to respond, and faster responses can therefore be expected by scaling down the valve dimensions. However, we must also bear in mind that the obtained flow rates only require a rather small expansion and contraction of the gel, involving the region immediately in contact with the external solution, and the full dimension of the valve therefore are not implicit in producing the response. Recent advances in multi-photon polymerization instrumentation now enable these responsive gels to be created at much higher resolution, and in much more complex 3D spatial designs. The resulting gel structures exhibit swelling/contraction kinetics that are orders of magnitude faster than the values reported herein. This also means that larger micron-scale gel actuators can be assembled from an arrangement of much smaller nano-scale sub-units each of which expand and contract at a rate orders of magnitude faster than an equivalent single monolithic micron-scale actuator (Tudor et al., 2018).

As these actuators can be photopolymerized in pre-fabricated channels from liquid precursors, and subsequently controlled using light sources located outside the fluidic system; (i.e., the control layer is physically separate from the fluidic layer), the responsive features can be integrated without disrupting the way the fluidic system is produced. Therefore, flexible flow regulation can now be integrated at multiple locations, as the actuators are fully integrated into the fluidic system, with no need to incorporate physical contact between the stimulus source and the actuator (no electronic contacts are required—the control layer can be completely separate from the fluidic layer). In contrast, conventional valves comprise a bottleneck to increasing fluidic complexity, as scaling up is complex, expensive, inflexible, costly and technically very demanding. Furthermore, the actuator form and mode of action of the polymer actuators can be varied, for example, by coating the fluidic channel walls (channel inner diameter becomes variable), or having predesigned shapes (e.g., pillars, wedges) emerge and retreat into walls under external photocontrol.

While this paper focuses on photo-responsive gels, stimuli can be thermal, magnetic, electrochemical, or molecular. Molecular responsive fluidic systems are particularly interesting, as this could form the basis of a completely materials based responsive system, totally self-contained, in

which the control function is determined completely at the materials level, with no need for electronics, power, or external connectivity. This can be achieved by using gels incorporating binding sites for a particular molecular target that swell and contract in response to changes in the concentration of the molecular target in the external solution (Bruen et al., 2020). Ultimately, polymers that inherently actuate in response to changes in their molecular environment will provide the basis for futuristic fluidics that can implement sophisticated flow control without recourse to electronics and external intervention, i.e., the fluidic system will control its own behavior. Systems exhibiting such autonomous control characteristics are the key to creating completely new approaches to molecular sensing and delivery platforms with capabilities far beyond that currently possible.

DATA AVAILABILITY STATEMENT

The original contributions presented in the study are included in the article/**Supplementary Material**, further inquiries can be directed to the corresponding authors.

AUTHOR CONTRIBUTIONS

KP was responsible for development of the synthetic method used to make the SP photoswitch, demonstrating scale up and consistency with green chemistry principles. RB was responsible for producing the electronics and chip alignment system, and for implementing the PID algorithm. MM was responsible for design and implementation of the bench flow-control experiments and characterization of the photovalve response. All of the above contributed to writing of the manuscript. DD was responsible for the overall concept and creating the integrated version of the manuscript.

FUNDING

We wish to acknowledge funding from the European Commission through the Holifab project, Grant number 760927 (H2020-NMBP-PILOTS-2017), and from Science Foundation Ireland (SFI) through the INSIGHT Center, Grant Number SFI/12/RC/2289-P2, co-funded by the European Regional Development Fund.

ACKNOWLEDGMENTS

We thank Dr. J. ter Schiphorst and Dr. A. Schenning (TU Eindhoven) for their valuable previous collaborations and discussions. Laser cutting was carried out at the Nano Research Facility in Dublin City University, which was funded under the Program for Research in Third Level Institutions (PRTLI) Cycle 5. The PRTLI is co-funded through the European Regional Development Fund (ERDF), part of the European Union Structural Funds Program 2011–2015.

SUPPLEMENTARY MATERIAL

The Supplementary Material for this article can be found online at: https://www.frontiersin.org/articles/10.3389/fmats.2020.615021/full#supplementary-material.

REFERENCES

Abdollahi, A., Alinejad, Z., and Mahdavian, A. R. (2017). Facile and fast photosensing of polarity by stimuli-responsive materials based on spiropyran for reusable sensors: a physico-chemical study on the interactions. *J. Mater. Chem. C.* 5 (26), 6588–6600. doi:10.1039/c7tc02232h

Balmond, E. I., Tautges, B. K., Faulkner, A. L., Or, V. W., Hodur, B. M., Shaw, J. T., et al. (2016). Comparative evaluation of substituent effect on the photochromic properties of spiropyrans and spirooxazines. *J. Org. Chem.* 81 (19), 8744–8758. doi:10.1021/acs.joc.6b01193

Bruen, D., Delaney, C., Chung, J., Ruberu, K., Wallace, G. G., Diamond, D., et al. (2020). 3D printed sugar-sensing hydrogels. *Macromol. Rapid Commun.* 41 (9), 1900610. doi:10.1002/marc.201900610

Byrne, R., and Diamond, D. (2006). Chemo/bio-sensor networks. *Nat. Mater.* 5 (6), 421–424. doi:10.1038/nmat1661

Campos, P. P., Dunne, A., Delaney, C., Moloney, C., Moulton, S. E., Benito-Lopez, F., et al. (2018). Photoswitchable layer-by-layer coatings based on photochromic polynorbornenes bearing spiropyran side groups. *Langmuir* 34 (14), 4210–4216. doi:10.1021/acs.langmuir.8b00137

Chen, L., Zhu, Y., Yang, D., Zou, R., Wu, J., and Tian, H. (2014). Synthesis and antibacterial activities of antibacterial peptides with a spiropyran fluorescence probe. *Sci. Rep.* 4 (1), 6860. doi:10.1038/srep06860

Chen, S., Gao, Y., Cao, Z., Wu, B., Wang, L., Wang, H., et al. (2016). Nanocomposites of spiropyran-functionalized polymers and upconversion nanoparticles for controlled release stimulated by near-infrared light and PH. *Macromolecules* 49 (19), 7490–7496. doi:10.1021/acs.macromol.6b01760

Coleman, S., Ter Schiphorst, J., Ben Azouz, A., Bakker, S., Schenning, A. P. H. J., and Diamond, D. (2017). Tuning microfluidic flow by pulsed light oscillating spiropyran-based polymer hydrogel valves. *Sensor. Actuator. B Chem.* 245, 81–86. doi:10.1016/j.snb.2017.01.112

Czugala, M., O'Connell, C., Blin, C., Fischer, P., Kevin, J., Fraser, K. J., et al. (2014). Swelling and shrinking behaviour of photoresponsive phosphonium-based ionogel microstructures. *Sensor. Actuator. B Chem.* 194, 105–113. doi:10.1016/j.snb.2013.12.072

Delaney, C., McCluskey, P., Coleman, S., Whyte, J., Kent, N., and Diamond, D. (2017). Precision control of flow rate in microfluidic channels using photoresponsive soft polymer actuators. *Lab Chip* 17, 2013–2021. doi:10.1039/C7LC00368D

Donohoe, A., Lacour, G., Harrison, D. J., Diamond, D., and McCaul, M. (2019). Fabrication of rugged and reliable fluidic chips for autonomous environmental analyzers using combined thermal and pressure bonding of polymethyl methacrylate layers. *ACS Omega* 4 (25), 21131–21140. doi:10.1021/acsomega.9b01918

Dou, Q., Low, Z. W. K., Zhang, K., and Loh, X. J. (2017). A new light triggered approach to develop a micro porous tough hydrogel. *RSC Adv.* 7 (44), 27449–27453. doi:10.1039/c7ra03214e

Dunne, A., Delaney, C., Florea, L., and Diamond, D. (2016a). Solvato-morphologically controlled, reversible NIPAAm hydrogel photoactuators. *RSC Adv.* 6 (86), 83296–83302. doi:10.1039/C6RA16807H

Dunne, A., Delaney, C., Florea, L., and Diamond, D. (2016b). Solvato-morphologically controlled, reversible NIPAAm hydrogel photoactuators. *RSC Adv.* 6 (86), 83296–83302. doi:10.1039/c6ra16807h

Fischer, E., and Hirshberg, Y. (1952). formation of coloured forms of spirans by low-temperature irradiation. *J. Chem. Soc.* (NOV), 4522–4524.

Florea, L., Diamond, D., and Benito-Lopez, F. (2012). Photo-responsive polymeric structures based on spiropyran. *Macromol. Mater. Eng.* 297 (12), 1148–1159. doi:10.1002/mame.201200306

Han, S., and Chen, Y. (2011). Mercury ion induced activation of the C-O bond in a photo-responsive spiropyran. *Dyes Pigments* 88 (3), 235–239. doi:10.1016/j.dyepig.2010.06.011

Jalani, G., Naccache, R., Rosenzweig, D. H., Haglund, L., Vetrone, F., and Cerruti, M. (2016). Photocleavable hydrogel-coated upconverting nanoparticles: a multifunctional theranostic platform for NIR imaging and on-demand macromolecular delivery. *J. Am. Chem. Soc.* 138 (3), 1078–1083. doi:10.1021/jacs.5b12357

Karimi, M., Sahandi Zangabad, P., Baghaee-Ravari, S., Ghazadeh, M., Mirshekari, H., and Hamblin, M. R. (2017). Smart nanostructures for cargo delivery: uncaging and activating by light. *J. Am. Chem. Soc.* 139 (13), 4584–4610. doi:10.1021/jacs.6b08313

Kawata, S., and Kawata, Y. (2000). Three-dimensional optical data storage using photochromic materials. *Chem. Rev.* 100 (5), 1777–1788. doi:10.1021/cr980073p

Keum, S. R., Lee, K. B., Kazmaier, P. M., and Buncel, E. (1994). "A novel method for measurement of the merocyanine-spiropyran interconversion in the non-activated 1,3,3-trimethylspiro-(2H-1-Benzospiran-2,2'-Indoline) derivatives. *Tetrahedron Lett.* 35 (7), 1015–1018. doi:10.1016/S0040-4039(00)79953-9

Klajn, R. (2014). Spiropyran-based dynamic materials. *Chem. Soc. Rev.* 43 (1), 148–184. doi:10.1039/C3CS60181A

Kocer, A., Walko, M., Meijberg, W., and Feringa, B. L. (2005). A light-actuated nanovalve derived from a channel protein. *Science* 309 (5735), 755–758. doi:10.1126/science.1114760

Lee, C. K., Beiermann, B. A., Silberstein, M. N., Wang, J., Moore, J. S., Sottos, N. R., et al. (2013). Exploiting force sensitive spiropyrans as molecular level probes. *Macromolecules* 46 (10), 3746–3752. doi:10.1021/ma4005428

Li, W., Trosien, S., Schenderlein, H., Graf, M., and Biesalski, M. (2016). Preparation of photochromic paper, using fibre attached spiropyran polymer networks. *RSC Adv.* 6 (111), 109514–109518. doi:10.1039/c6ra23673a

Lukyanov, B. S., and Lukyanova, M. B. (2005). Spiropyrans: synthesis, properties, and application. (Review). *Chem. Heterocycl. Compd.* 41 (3), 281–311. doi:10.1007/s10593-005-0148-x

Matczyszyn, K., Olesiak-Banska, J., Nakatani, K., Yu, P., Murugan, N. A., Zaleśny, R., et al. (2015). One- and two-photon absorption of a spiropyran-merocyanine system: experimental and theoretical studies. *J. Phys. Chem. B.* 119 (4), 1515–1522. doi:10.1021/jp5071715

Minkin, V. I. (2004). Photo-, thermo-, solvato-, and electrochromic spiroheterocyclic compounds. *Chem. Rev.* 104 (5), 2751–2776. doi:10.1021/cr020088u

Ozhogin, I. V., Chernyavina, V. V., Lukyanov, B. S., Malay, V. I., Rostovtseva, I. A., Makarova, N. I., et al. (2019). Synthesis and study of new photochromic spiropyrans modified with carboxylic and aldehyde substituents. *J. Mol. Struct.* 1196, 409–416. doi:10.1016/j.molstruc.2019.06.094

Porter, T., Stewart, R., Reed, J., and Morton, K. (2007). Models of hydrogel swelling with applications to hydration sensing. *Sensors* 7 (9), 1980–1991. doi:10.3390/s7091980

Rosario, R., Gust, D., Hayes, M., Jahnke, F., Springer, J., and Garcia, A. A. (2002). Photon-modulated wettability changes on spiropyran-coated surfaces. *Langmuir* 18 (21), 8062–8069. doi:10.1021/la025963l

Satoh, T., Sumaru, K., Takagi, T., Takai, K., and Kanamori, T. (2011). Isomerization of spirobenzopyrans bearing electron-donating and electron-withdrawing groups in acidic aqueous solutions. *Phys. Chem. Chem. Phys.* 13 (16), 7322. doi:10.1039/c0cp01989e

Schiphorst, J. T., Coleman, S., Stumpel, J. E., Ben Azouz, A., Diamond, D., Schenning, A. P., et al. (2015). Molecular design of light-responsive hydrogels, for *in Situ* generation of fast and reversible valves for microfluidic applications. *Chem. Mater.* 27 (17), 5925–5931. doi:10.1021/acs.chemmater.5b01860

Schiphorst, J. T., van den Broek, M., de Koning, T., Murphy, J. N., Schenning, A. P. H. J., and Esteves, A. C. C. (2016). Dual light and temperature responsive cotton fabric functionalized with a surface-grafted spiropyran-NIPAAm-hydrogel. *J. Mater. Chem.* 4 (22), 8676–8681. doi:10.1039/c6ta00161k

Schiphorst, J. T., Saez, J., Diamond, D., Benito-Lopez, F., and Schenning, A. P. H. J. (2018). Light-responsive polymers for microfluidic applications. *Lab Chip* 18 (5), 699–709. doi:10.1039/C7LC01297G

Seefeldt, B., Kasper, R., Beining, M., Mattay, J., Arden-Jacob, J., Kemnitzer, N., et al. (2010). Spiropyrans as molecular optical switches. *Photochem. Photobiol. Sci.* 9 (2), 213. doi:10.1039/b9pp00118b

Shao, N., Jin, J., Wang, H., Zheng, J., Yang, R., Chan, W., et al. (2010). Design of bis-spiropyran ligands as dipolar molecule receptors and application to *in Vivo* glutathione fluorescent probes. *J. Am. Chem. Soc.* 132 (2), 725–736. doi:10.1021/ja908215t

Sugiura, S., Szilágyi, A., Sumaru, K., Hattori, K., Takagi, T., Filipcsei, G., et al. (2009). On-demand microfluidic control by micropatterned light irradiation of a photoresponsive hydrogel sheet. *Lab Chip* 9 (2), 196–198. doi:10.1039/b810717c

Sugiura, S., Sumaru, K., Ohi, K., Hiroki, K., Takagi, T., and Kanamori, T. (2007). Photoresponsive polymer gel microvalves controlled by local light irradiation. *Sensor Actuator Phys.* 140 (2), 176–184. doi:10.1016/j.sna.2007.06.024

Sun, Z., Liu, S., Li, K., Tan, L., Cen, L., and Fu, G. (2016). Well-defined and biocompatible hydrogels with toughening and reversible photoresponsive properties. *Soft Matter* 12 (7), 2192–2199. doi:10.1039/c5sm02129d

Tan, B.-H., Yoshio, M., Ichikawa, T., Mukai, T., Ohno, H., and Kato, T. (2006). Spiropyran-based liquid crystals: the Formation of columnar phases via acid-induced spiro-merocyanine isomerisation. *Chem. Commun.* 45, 4703–4705. doi:10.1039/b610903a

Tudor, A., Delaney, C., Zhang, H., Thompson, A. J., Curto, V. F., and Yang, G.-Z. (2018). Fabrication of soft, stimulus-responsive structures with sub-micron resolution via two-photon polymerization of poly(ionic Liquid)s. *Mater. Today* 21 (8), 807–816. doi:10.1016/j.mattod.2018.07.017

Vidaysky, Y., Yang, S. J., Abel, B. A., Agami, I., Diesendruck, C. E., Coates, G. W., et al. (2019). Enabling room-temperature mechanochromic activation in a glassy polymer: synthesis and characterization of spiropyran polycarbonate. *J. Am. Chem. Soc.* 141 (25), 10060–10067. doi:10.1021/jacs.9b04229

Wagner, K., Byrne, R., Zanoni, M., Gambhir, S., Dennany, L., Breukers, R., et al. (2011). A multiswitchable poly(terthiophene) bearing a spiropyran functionality: understanding photo- and electrochemical control. *J. Am. Chem. Soc.* 133 (14), 5453–5462. doi:10.1021/ja1114634

Wang, B., Xiao, X., Zhang, Y., and Liao, L. (2019). High strength dual-crosslinked hydrogels with photo-switchable color changing behavior. *Eur. Polym. J.* 116, 545–553. doi:10.1016/j.eurpolymj.2019.04.035

Xia, H., Xie, K., and Zou, G. (2017). Advances in spiropyrans/spirooxazines and applications based on fluorescence resonance energy transfer (FRET) with fluorescent materials. *Molecules* 22 (12). doi:10.3390/molecules22122236

Xie, X., Mistlberger, G., and Bakker, E. (2012). Reversible photodynamic chloride-selective sensor based on photochromic spiropyran. *J. Am. Chem. Soc.* 134 (41), 16929–16932. doi:10.1021/ja307037z

Yagi, S., Nakamura, S., Watanabe, D., and Nakazumi, H. (2009). Colorimetric sensing of metal ions by bis(spiropyran) podands: towards naked-eye detection of alkaline earth metal ions. *Dyes Pigments* 80 (1), 98–105. doi:10.1016/j.dyepig.2008.05.012

Zhang, D., Shah, P. K., Culver, H. R., David, S. N., Stansbury, J. W., Yin, X., et al. (2019a). Photo-responsive liposomes composed of spiropyran-containing triazole-phosphatidylcholine: investigation of merocyanine-stacking effects on liposome-fiber assembly-transition. *Soft Matter* 15 (18), 3740–3750. doi:10.1039/c8sm02181c

Zhang, L., Deng, Y., Tang, Z., Zheng, N., Zhang, C., Xie, C., et al. (2019b). One-pot synthesis of spiropyrans. *Asian J. Org. Chem.* 8 (10), 1866–1869. doi:10.1002/ajoc.201900488

Ziolkowski, B., Florea, L., Theobald, J., Benito-Lopez, F., and Diamond, D. (2013). Self-protonating spiropyran-Co-NIPAM-Co-acrylic acid hydrogel photoactuators. *Soft Matter* 9 (36), 8754–8760. doi:10.1039/c3sm51386f

Ziółkowski, B., Florea, L., Theobald, J., Benito-Lopez, F., and Diamond, D. (2016). Porous self-protonating spiropyran-based NIPAAm gels with improved reswelling kinetics. *J. Mater. Sci.* 51 (3), 1392–1399. doi:10.1007/s10853-015-9458-2

Conflict of Interest: The authors declare that the research was conducted in the absence of any commercial or financial relationships that could be construed as a potential conflict of interest.